processes

MDPI

Article

Competitive Cation Adsorption on Electron-Irradiated Sheep Wool Changes the Fitting of Adsorption Isotherms for Single-Component Solutions

Mária Porubská *, Karin Koóšová and Jana Braniša

Department of Chemistry, Faculty of Natural Sciences and Informatics, Constantine the Philosopher University in Nitra, Tr. A. Hlinku 1, 949 74 Nitra, Slovakia

* Correspondence: mporubska@ukf.sk; Tel.: +421-37-6408-655

Abstract: This work analyses 10 adsorption isotherm models applied to adsorption of Cr(III) and Cu(II) from binary solutions on electron-irradiated sheep wool (0-24-100) kGy. The results are compared with fitting the same adsorbates from corresponding single solutions. The competing cation significantly changes the fitting of the selected isotherms to the extent that even simultaneous fitting of the same cation in the single and binary solution is rare. In the case of Cr(III), 4 favourable matches were found out of 30 compared cases, while in the case of Cu(II), only 2 conformities were found. Having the Cr(III) coordination number exclusively of 6, but Cu(II) up to 4, 5, 6, the last coordinates more easily with the ligands provided by keratin, resulting in preferential chemisorption. If there is still a lack of cysteic acid in the wool to interact with Cr(III) also, this is adsorbed on the wool physically, too. The amount of cysteic acid increasing in the wool with the absorbed dose of energy improves the chemisorption of Cr(III), as well. It can be summarized that during competitive adsorption, Cu(II) binds by chemisorption and Cr(III) by both physisorption and chemisorption, depending on the dose of energy absorbed by the wool.

Keywords: sheep wool; electron beam irradiation; Cr(III); Cu(II); competitive adsorption; fitting adsorption isotherms

check for updates

Citation: Porubská, M.; Koóšová, K.; Braniša, J. Competitive Cation Adsorption on Electron-Irradiated Sheep Wool Changes the Fitting of Adsorption Isotherms for Single-Component Solutions. *Processes* **2023**, *11*, 502. https://doi.org/10.3390/pr11020502

Academic Editor: Anil K. Bhowmick

Received: 4 January 2023
Revised: 24 January 2023
Accepted: 4 February 2023
Published: 7 February 2023

1. Introduction

The removing of pollutants from the aquatic environment by adsorption on waste biomass can solve two problems at the same time: on the one hand, obtaining cheap usable material, and on the other hand, reducing the volume of waste. In most cases, in practice, this involves adsorption from multicomponent solutions. Here, unpredictable interactions can be expected, and describing such processes is not easy. This corresponds to the smaller number of studies dealing with adsorption from binary or multicomponent solutions compared to single ones. Research is most often focused on the elimination of heavy metals from multicomponent solutions by adsorption on adsorbents of plant origin. It is possible to find data on the elimination of Cu(II), Pb(II), Cd(II), and Ni(II) in various combinations; data obtained for Zn(II), Co(II), and Hg(II), but also Cr(VI) and both As(III) and Au(III) are described. It is significant that the indicated adsorption characteristics refer to already optimized processes, which are difficult to set on an industrial scale. The problem is that the optimal adsorption conditions are not the same for all present solutes, e.g., if one component requires a different pH or concentration ratio than others. In general, this problem is considered quite difficult. This is the reason why various modifications of "standard" isothermal models are being developed, including further corrections of the basic models to achieve agreement with the experimental results. Although the exact analysis of the adsorption data of the applied cations is not reliable due to the different conditions of the conducted processes, it nevertheless makes it possible to formulate at least approximative trends.

The Cu(II) cation is part of the systems investigated in works [1–6], with the prevailing conclusion that Cu(II) is adsorbed better than the other components. Articles [7–12] focus on the adsorption of Pb(II) accompanied by other components. This cation is favoured in the studied systems due to its atom size and causes a strong concentration-dependent antagonistic effect on the removal of Cd(II) and Ni(II) in binary mixtures [7,8]. The competitive adsorption of Cd(II) was also tested in studies [1–5,9,11,13]. In the order of adsorption partners, the Cd(II) appears in the middle of other cations. Its sorption capacity alternates with Ni(II) as a co-component [3–5,7,13], but the results vary according to the process conditions. Fewer data can be found for Zn(II) [2,10], Hg(II) [8,10], Cr(VI) [14,15], As(III) [16], or Co(II) [12].

The above-mentioned articles describe the use of biosorbent materials of plant origin. Information about the use of adsorbents of animal origin is very sporadic and includes only native sheep wool [17–21] or physico-chemically modified wool [22,23]. These studies deal exclusively with single-component solutions. On the other hand, information on adsorption on wool from multicomponent solutions is very rare, if any, and only evaluates the adsorption of the dominant cation under laboratory-optimized conditions [24]. The little attention given to sheep wool as an adsorbent is somewhat surprising, since there is an abundance of sheep wool unsuitable for textile use.

Chemical-free modified sheep wool is a relatively new promising adsorbent, which we are currently dealing with [25]. The modification is a dry process of irradiating sheep wool with an accelerated electron beam without producing wastewater. The induced change in the primary and secondary structure of keratin provoked its interesting adsorption properties [26–29]. It was found that the results depended not only on the absorbed energy dose, but also on the pre-exposure [30] and post-exposure conditions [31,32]. The experimental results for the adsorption of Cr(III) and Cu(II) from single solutions were tested to fit 10 isothermal adsorption models [33,34]. Considering practical conditions involving separation adsorption from multicomponent solutions, we also investigated competitive adsorption from a binary solution containing Cr(III) and Cu(II). An unexpected and interesting observation was that by changing the dose of energy absorbed by the wool, there was a change in the preferential adsorption from Cu(II) to Cr(III) [35]. These peculiarities, together with the spatial conditions inside the keratin chains of native or exposed wool, can play a determining role in competitive adsorption. Therefore, in the presented study, we want to analyse the effect of the adsorption of these cations from single and binary solutions on the fitting of 10 selected adsorption isotherms for individual dosed wool samples. Linearized dependences of the models have so far been interpreted only on the basis of the correlation of expected straight lines with the experimental data, without a next deeper statistical analysis. The goal was to get some primary information that will be developed in further research. The obtained data can be used not only for the removal of unwanted pollutants from the aquatic environment, but also for the separation of recyclable components from industrial waste. They can also be a good starting point to obtain the elements necessary for the production of microchips, the lack of which will affect the automotive industry, the production of computers, smartphones, graphics, and payment cards, or the issuing of cards needed for electronic communication with institutions.

2. Materials and Methods

2.1. Materials

The sheep wool came from the spring sheep-shearing (2018) of a Merino–Suffolk crossbreed bred in a region of Central Slovakia. The fibre thickness was in the range of 27–33 μm. The wool was scoured in tap water using ultrasonic bath (K5LE, Kraintek, Podhájska, Slovakia), 3 × 10 min at 40 °C, dried freely, and irradiated in a UELR–5–1S linear electron accelerator (FGUP NIIEFA, Petersburg, Russia and operated by Progress Final Ltd., Slovakia) with installed energy of 5 MeV. The samples with absorbed doses of

(0–24–100) kGy were stored under common conditions and room temperature and used for sorption batch experiments.

The chemicals chromium potassium sulphate dodecahydrate $KCr(SO_4)_2 \cdot 12H_2O$ and copper sulphate pentahydrate $CuSO_4 \cdot 5H_2O$ were used as Cr(III) and Cu(II) adsorbates. All chemicals were supplied by Labo—SK Ltd. (Bratislava, Slovakia) in analytical grade.

2.2. Spectral Measurements

Spectrometer Specord 50 Plus (Analytikjena, Jena, Germany) with 1 cm cell was used to determine of Cr(III) (λ = 415 nm) and Cu(II) (λ = 809 nm) contents in the bath. The comparative sample was always the aqueous extract from the wool with absorbed dose corresponding to the measured sample, obtained after 24 h contact of the sample with deionized water under the same conditions.

Unlike single systems, determination of the Cr(III) equilibrium concentration (C_e) in binary solutions involved correcting the read absorbance for drift caused by Rayleigh scattering in the field of shorter wave lengths (415 nm) when the Cu(II) ions were present, increasing ionic strength I. Relevant correction in the Cr(III) absorbance was estimated as the difference between the Cr(III) absorbance read for the calibration sample containing also the Cu(II) and the single corresponding Cr(III) solution. This difference was subtracted from the Cr(III) absorbance values measured for the binary bath in equilibrium [35]. Absorbance of the Cu(II) was not affected by the Cr(III) ions since λ = 809 nm was out of the Rayleigh scattering condition in this case.

2.3. Adsorption Experiments

The testing solutions of both Cr(III) and Cu(II) salts in the concentration range of (15–35) mmol/L for the sorption experiments were prepared by diluting the corresponding stock solutions with demineralized water. The selected concentrations allow analysis using UV-VIS spectroscopy. In the case of binary systems, the Cr(III) calibration solutions were supplemented with Cu(II) and vice versa. Cu(II) calibration solutions were supplemented with Cr(III). More details can be found in Supplementary Materials.

The batch sorption experiments were conducted with both single Cr(III) and Cu(II) or binary solutions applying the corresponding above-mentioned concentrations. After being cut to 3–5 mm, 0.2 g of wool fibres were placed into a glass cup with a cap, and the testing solution of 20 mL in volume was added. The content of the glass cup was first shaken for 6 h at room temperature on a laboratory horizontal shaker (Witeg SHR–2D, Labortechnik GmbH, Wertheim, Germany) and then kept in static mode for the next 18 h. Then the remaining solution was filtered through KA5 filter paper and used for determination of residual Cr(III) or Co(II). Every sorption procedure was carried out in triplicate. The relative error of the equilibrium concentration did not exceed 10%.

The parameter q_e as a measure of wool sorptivity at equilibrium was calculated using the following Equation (1):

$$q_e = (x_1 - x_2)/m \quad (1)$$

where q_e is the sorptivity, defined as the equilibrium amount of sorbate in mg per 1 g of the sorbent for individual wool samples when particular testing solution is applied in the specified concentration, x_1 is the amount of the sorbate added in the initial solution (mg), x_2 is the residual equilibrium amount of the sorbate in the solution after its contact with the wool sample (mg), and m is the mass of the wool sample taken for analysis (g).

2.4. Testing of Isothermal Models

Ten isothermal models selected to examine whether they match the experimental data are summarized in Table 1. The data needed to calculate the parameters of the individual isothermal models were obtained from the graphic dependencies generated for each model, cation, and absorbed dose using Excel, also providing correlation equations for linearized relationships.

Table 1. The isotherm models selected, conditions of calculation, and plotting curves to test the experimental results fitting.

Isotherm Model	Linearized Equation	Plot of Dependence	Units Used for Calculation (C_0, C_e; q_e; Θ)
Langmuir [36]	$\frac{C_e}{q_e} = \frac{1}{Q \cdot K_L} + \frac{1}{Q} C_e$	C_e against C_e/q_e	mg/L; mg·g^{-1}
Freundlich [37]	$\log q_e = \log K_F + \frac{1}{n} \cdot \log C_e$	log C_e against log q_e	mg/L; mg·g^{-1}
Dubinin-Radushkevich [38]	$\ln q_e = \ln q_s - K_D \varepsilon^2$; $\varepsilon = RT \ln\left(1 + \frac{1}{C_e}\right)$	ε^2 against ln q_e	mol/L; mol·g^{-1}
Temkin [39]	$q_e = \frac{RT}{b} \ln K_T + \frac{RT}{b} \ln C_e$	ln C_e against q_e	mg/L; mg·g^{-1}
Flory-Huggins [40]	$\log\left(\frac{\theta}{C_0}\right) = \log K_{FH} + n \log(1 - \theta)$	log $(1 - \Theta)$ against log (Θ/C_0)	mol/L; mol·g^{-1}
Halsey [41]	$\ln\ q_e = \frac{1}{n_H} \ln K_H - \frac{1}{n_H} \ln C_{q_e}$	ln C_e against ln q_e	mg/L; mg·g^{-1}
Harkins-Jura [42]	$\frac{1}{q_e^2} = \frac{B}{A} - \left(\frac{1}{A}\right) \log C_e$	log C_e against $1/{q_e}^2$	mg/L; mg·g^{-1}
Jovanovic [43]	$\ln q_e = \ln q_{max} - K_J C_e$	C_e against ln q_e	mg/L; mg·g^{-1}
Elovich [44]	$\ln \frac{q_e}{C_e} = \ln K_E \cdot q_m - \frac{1}{q_m} q_e$	q_e against ln (q_e/C_e)	mg/L; mg·g^{-1}
Redlich-Peterson [45]	$\ln \frac{C_e}{q_e} = \beta\ \ln C_e - \ln A$	ln C_e against ln (C_e/q_e)	mg/L; mg·g^{-1}

Note: Meaning of basic symbols: C_e is concentration of solute at equilibrium, q_e is amount of adsorbate adsorbed at equilibrium, C_0 is solute initial concentration, Θ is degree of surface coverage.

3. Results and Discussion

The elements chromium and copper belong to the elements of the 4th period of the periodic table as the first series of transition elements (3D elements). Their valence orbital configuration is [Ar]3d^{5}4s^1 for Cr and [Ar] 3d^{10} 4s^1 for Cu, and that is why they tend to form complexes. Available ligands in keratin are amine/imine, hydroxyl, or SH groups providing good complexing conditions. Although both Cr(III) and Cu(II) are Lewis acids generating complex salts as carboxylates or cysteinates with ligands from keratin, their various compositions and architectures modify the adsorption differently. As showed in [28], the Cu(II) very readily forms complexes with the ligands provided by keratin, immediately on the surface of the fibre. Since native keratin contains more carboxyl groups than those amino ones [46], some parts of the Cu(II)-complex molecule have to be ligands coming from neighbouring keratin chains forming crosslinks, or, in the case of amorphous structure, the ligands may also be provided by the same chain. The formed network obstructs the entry of additional cations into the fibre volume, although electron beam irradiation creates potential conditions to form other complexes in the inner layers, as well.

As referred to [47], all chromium complexes without exception have a coordination number of 6 and an octahedral form, while Cu(II) complexes show the coordination number 4 and 6 most frequently. However, besides that, the Cu(II) complexes often exhibit a distorted tetrahedral or octahedral structure or, less frequently, a trigonal bipyramid having coordination number 5 [48].

In addition to the various compositions of keratin side functional groups, the chemical linking of a pair of chains through R-S-S-R disulphide bridges is characteristic, which is the reason for keratin insolubility in common solvents. Based on results from our previous studies [25,26], the wool with dose around 24 kGy shows certain anomalies. They can also be observed in some conspicuously "deviated" correlation coefficients in Table 2. The

absorption of such energetic dose by the wool is enough to break sulphide bridges [25,30], which yields the radical anion ($SS^{\bullet-}$), according to reaction (2):

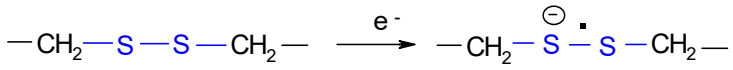

(2)

The unpaired electron in $SS^{\bullet-}$ resides in a three—electron σ—bond. Generally, radical anion $SS^{\bullet-}$ is highly reactive and, in the oxygenated environment, undergoes oxidation, although some parts may also recombine. The S-oxidation intermediates are cystine monoxide R-SO-S-R and cystine dioxide R-SO_2-S-R. In these products, the S-O bonds are strongly polarized toward oxygen. Being the strong hydrogen bond acceptors [49], their interaction with an adsorbate can vary. The final product of the cystine oxides transformation is cysteic acid. Thus, the higher the dose, the more acidic groups are in keratin, because the resulting cysteic acid R-SO_3H is added to the original carboxyl groups. Whereas the surface layers of the fibre are richer in sulphur content than the inner ones, the abundance of S-oxidized species will be near the surface, and these can modify the overall surface electric charge. Such physical-chemical structure of wool predetermines cations for chemisorption.

Table 2. The overview of the correlation of linearized equations calculated from the experimental results of the Cr(III) and Cu(II) adsorption on sheep wool irradiated with electron beam for selected isothermal models from single [33,34] and binary [35] systems.

Isotherm Model	Dose (kGy)	Correlation			
		Cr(III) Single	Cr(III) Binary	Cu(II) Single	Cu(II) Binary
Langmuir	0	R^2 = 0.6781	R^2 = 0.9891	R^2 = 0.9172	R^2 = 0.8701
	24	R^2 = 0.0845	R^2 = 0.3180	R^2 = 0.9822	R^2 = 0.6558
	100	R^2 = 0.8994	R^2 = 0.9930	R^2 = 0.9177	R^2 = 0.5331
Freundlich	0	R^2 =0.8983	R^2 = 0.8661	R^2 = 0.6195	R^2 = 0.0164
	24	R^2 =0.9616	R^2 = 0.9466	R^2 = 0.9248	R^2 = 0.0046
	100	R^2 =0.9914	R^2 = 0.0457	R^2 = 0.1323	R^2 = 0.8596
Dubinin-Radushkevich	0	R^2 = 0.8567	R^2 = 0.8897	R^2 = 0.6291	R^2 = 0.0050
	24	R^2 = 0.9374	R^2 = 0.9605	R^2 = 0.9195	R^2 = 0.0099
	100	R^2 = 0.9769	R^2 = 0.3866	R^2 = 0.0902	R^2 = 0.8603
Temkin	0	R^2 = 0.8835	R^2 = 0.8329	R^2 = 0.5587	R^2 = 0.0092
	24	R^2 = 0.8083	R^2 = 0.9535	R^2 = 0.9136	R^2 = 0.0017
	100	R^2 = 0.8862	R^2 = 0.0514	R^2 = 0.1045	R^2 = 0.7205
Flory-Huggins	0	R^2 = 0.2373	R^2 = 0.923	R^2 = 0.9421	R^2 = 0.9871
	24	R^2 = 0.0002	R^2 = 0.3659	R^2 = 0.9576	R^2 = 0.9492
	100	R^2 = 0.5799	R^2 = 0.9652	R^2 = 0.9869	R^2 = 0.1603
Halsey	0	R^2 =0.8955	R^2 = 0.8667	R^2 = 0.6195	R^2 = 0.0164
	24	R^2 =0.9613	R^2 = 0.9466	R^2 = 0.9248	R^2 = 0.0046
	100	R^2 =0.9914	R^2 = 0.0475	R^2 = 0.1323	R^2 = 0.8596
Harkins-Jura	0	R^2 = 0.9858	R^2 = 0.9100	R^2 = 0.7135	R^2 = 0.0383
	24	R^2 = 0.9404	R^2 = 0.8812	R^2 = 0.9438	R^2 = 0.0113
	100	R^2 = 0.8826	R^2 = 0.0404	R^2 = 0.2051	R^2 = 0.7312
Jovanovic	0	R^2 = 0.9774	R^2 = 0.7624	R^2 = 0.5128	R^2 = 0.0578
	24	R^2 = 0.993	R^2 = 0.8829	R^2 = 0.8554	R^2 = 0.0021
	100	R^2 = 0.9888	R^2 = 0.009	R^2 = 0.2985	R^2 = 0.8467
Elovich	0	R^2 = 0.8471	R^2 = 0.9268	R^2 = 0.2946	R^2 = 0.1833
	24	R^2 = 0.3114	R^2 = 0.0736	R^2 = 0.8305	R^2 = 0.2369
	100	R^2 = 0.9587	R^2 = 0.0948	R^2 = 0.356	R^2 = 0.8509
Redlich-Peterson	0	R^2 = 0.3621	R^2 = 0.9775	R^2 = 0.9284	R^2 = 0.8844
	24	R^2 = 0.019	R^2 = 0.2074	R^2 = 0.9841	R^2 = 0.7967
	100	R^2 = 0.7328	R^2 = 0.9929	R^2 = 0.9067	R^2 = 0.5534

When studying adsorbent–adsorbate interactions, mathematical models of individual adsorption isotherms represent suitable additional information to ascertain the proposed

adsorption mechanism. They can also inspire a better interpretation of the observed facts. At the same time, they can indicate the character and efficiency of the adsorbent. The results of our adsorption experiments for the adsorption of Cr(III) and Cu(II) from mixed solutions on sheep wool irradiated with an electron beam [35] were tested for compliance with 10 models of adsorption isotherms, confronting the results with fitting of each cation from the single solutions.

To analyse the effect of the competing cation on the Cr(III) or Cu(II) adsorption, we used the corresponding constructed linearized equations (Table 1). Data for the single Cr(III) solutions [33] were compared with the results of the Cr(III) from binary solutions containing competing Cu(II) [35], and conversely, adsorption of Cu(II) from the single solution [34] is confronted with adsorption of the Cu(II) from solutions in the presence of Cr(III) [35].

The correlation factor R^2 resulting from the linear trend curve is generally considered to be the degree of conformity of the experimental data with the model. An overview of the resulting correlation coefficients for the analysed systems is presented in Table 2.

As can be seen from Table 2, the scattering of the R^2 coefficient is very large. For a simple classification of the data, we predetermined the correlation parameter $R^2 \geq 0.90$ as fitting and R^2 <0.85–0.89> as quasi-fitting to the given model. As resulted from Table 2, simultaneous fitting for the Cr(III) single and binary systems is not observed for any model in the whole dose range. Rarely, agreement can be found for selected doses, fully for 24 kGy in the Freundlich and Halsey model, as well as for 0 kGy in the Harkins–Jura model. Quasi-fitting shows the Langmuir model at the 100 kGy dose, the Freundlich and Halsey model at 0 kGy, and the Harkins–Jura and Jovanovic models at the 24 kGy sample. In the case of the single and binary Cu(II) solutions, full fitting is observed only with the Flory–Huggins model for two samples, namely for 0 and 24 kGy. A quasi-fit is still shown by the 0 kGy sample with the Redlich–Peterson model. In summary, it is possible to state greater deviations between the single and binary systems in the adsorption of the Cu(II) than for the Cr(III). The variability of compliance of the experimental data with the selected models applied to the corresponding single and binary systems is demonstrated in the graphic display of the individual isothermal models, where the dotted lines represent the trend-linearized dependence (Figures 1–10).

3.1. Langmuir Model

The Langmuir model is generally suitable for a homogeneous single-layer adsorption, where each active site has the same affinity for the adsorbate. Thus, the Langmuir model can be viewed as a characterization of the topology of the surface layer on the adsorbent. Graphic processing of the experimental results is shown in Figure 1.

3.1.1. Adsorption from Single Solutions

In the single Cr(III) system, the selective coordination number of Cr(III) limits the local formation of the complex on the surface of both native and irradiated wools because there are more types of acid groups, which leads to layer inhomogeneity (Table 2, Figure 1). The situation becomes even more complicated for 24 kGy wool, when the splitting of S-S bonds begins, and thus, the variety of interaction products increases, accompanied by a strong deviation from fitting. The homogeneity of the surface increased for the dose of 100 kGy, when more cysteic acid was produced from the S-S bonds split, but the carboxyl representation remained the same. The subsequent predominance of the formed Cr(III)-cysteinate improved the homogeneity of the surface, which is indicated by the model fitting already at the quasi-fitting level.

On the other hand, Cu(II) is more easily adsorbed on the wool surface due to several options for the construction of the Cu-complex, thus forming a more homogeneous surface at all doses. This corresponds to its conformity with the Langmuir model for all samples.

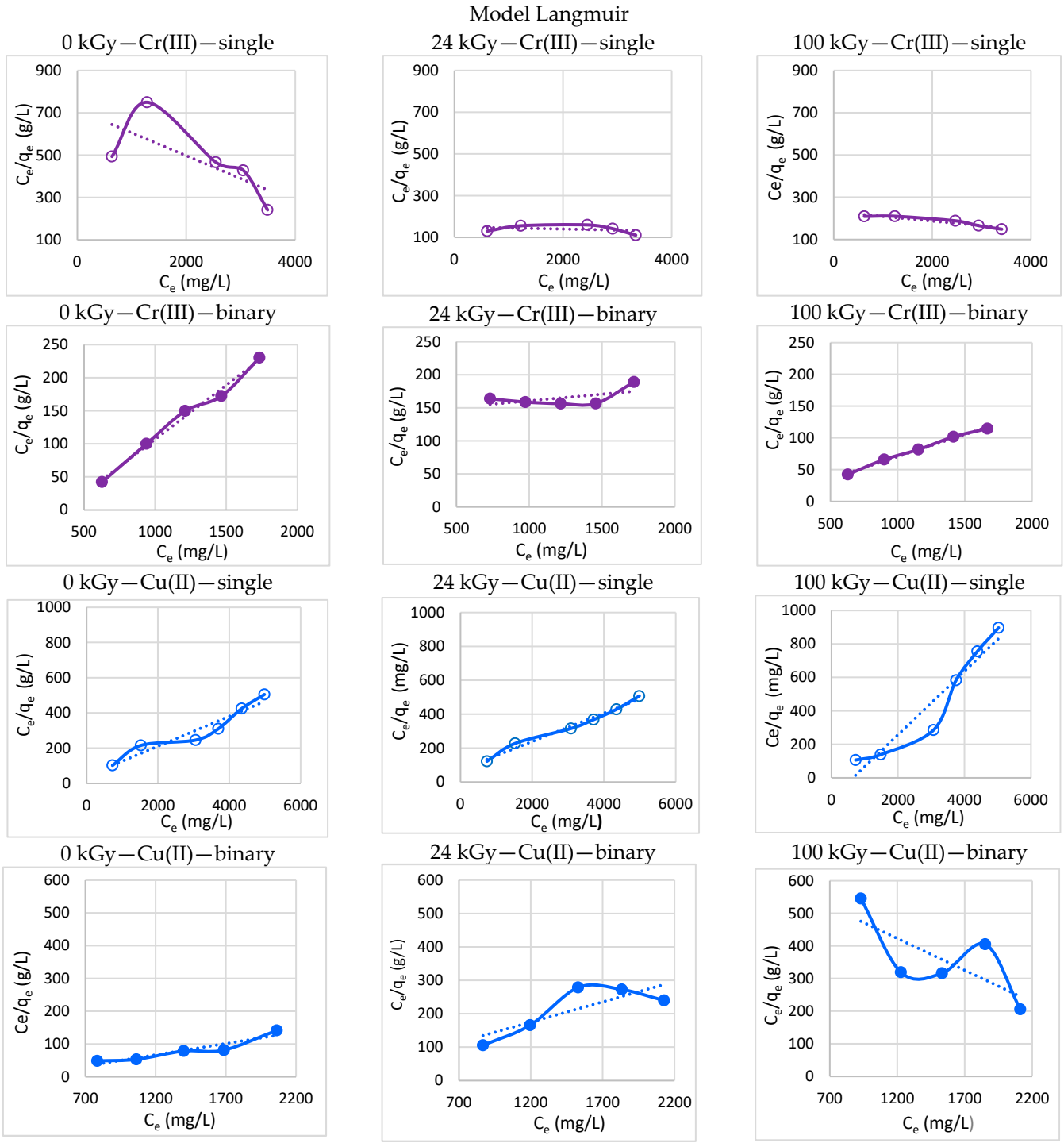

Figure 1. Langmuir charts of processed experimental data for Cr(III) and Cu(II) for both single and binary systems.

3.1.2. Adsorption from Binary Solutions

The situation changes in the binary solutions. Based on the result of the fitting in the binary system, it can be concluded that the homogeneous adsorbed layer on both the native and 100 kGy irradiated wool is formed by the Cr(III), but not by the Cu-complex. However, fitting this model for the binary Cr(III) does not mean that a larger mass of the Cr(III) is adsorbed on the surface of the wool, but that it is more homogeneous. As found in [35], the non-irradiated wool showed a higher sorptivity q_e for the Cu(II) at the 24 kGy dosed wool

sorptivity of both Cr(III) and Cu(II) cations converged without fitting. The 100 kGy sample showed the sorptivity of Cr(III) over Cu(II) (see Supplementary Materials).

For the 0 kGy dosed sample, the indicated homogeneity of the Cr(III) adsorption layer is caused by a cooperative adsorption of the Cr(III) [50], despite the dominance of sorptivity for the Cu(II). The side groups of the keratin constitutional amino acids have a bidentate potential, i.e., have at least two functional groups—donors capable of coordination with a central cation. Yet, according to space and energy conditions, one group can be capable of co-ordinating with the Cu(II), the other with the Cr(III). This is a case of co-operative adsorption. Since the number of suitable active sites for the co-operative adsorption of the Cr(III) is less, the Cr(III) layer is indeed homogeneous, but the mass of the adsorbed Cr(III) is smaller. In terms of the Cu(II), such a situation disturbs the homogeneity of the surface, and compared to the single Cu(II), the correlation coefficient indicates only quasi-fitting (Table 2).

At wool doses of 24 kGy, the -S-S- bonds between the couple of chains in the helix are already broken, and the formation of cystine oxides and cysteic acid starts on the resulting radicals. Disruption of the keratin structure facilitates the access of the solute inside of the biopolymer bulk. While the original amount of carboxyl groups remains unchanged and probably mostly occupied by the copper, the added S-oxidized groups are available for salt formation also with the Cr(III). A more balanced competition for the coordination site results in the convergence of both cations sorptivities [35] and the inhomogeneity of the layer, which causes a deviation from the fitting of the Langmuir model for both cations.

The sample of 100 kGy dosed wool in the binary system shows not only a homogeneous layer for the Cr(III), but also a higher sorptivity than the Cu(II) [35]. The higher the dose absorbed by the wool, the more S-S bonds were broken and the more cysteic acid is generated. The predominance of sorptivity for the Cr(III) over the Cu(II) in this case indicates a higher affinity of the Cr(III) to cysteic acid than the Cu(II). This can be caused by the capture of the main part of the Cu(II) already on the surface of the fibre, and the rest is not sufficient for a more significant penetration of the Cu-cations into the disturbed bulk. However, a higher positive charge density on smaller Cr(III) than Cu(II) can also play a role, and the formation of Cr(III)-cysteinate is preferred. This opinion is supported by a model interaction of the amino acid keratin—arginine with the Cr(III) and the Cu(II) in solutions. While the addition of the Cr(III) to an arginine solution resulted in the formation of Cr-arginate precipitate, the reaction of an equimolar solution of the Cu(II) with arginine gave a blue soluble complex with a shift from λ_{max0} = 809 nm in the single Cu(II) to a shorter wavelength in the binary solution with λ_{max1} = 705 nm. At the same time, the absorbance increased significantly from A_0 = 0.25 to A_1 = 0.61 [27], thus a hyper-blue shift occurred.

3.2. Freundlich Model

Unlike the Langmuir isotherm, the Freundlich model is not restricted to the formation of a monolayer. It can be applied to heterogeneous surfaces and multilayer adsorption. Charts for our data are displayed in Figure 2.

3.2.1. Adsorption from Single Solutions

From our data (Table 2, Figure 2), it is apparent that the Freundlich model for adsorption of the Cr(III) from the single system is suitable for the irradiated wool samples (24 and 100 kGy), and the non-irradiated wool only quasi-fits. The satisfying correlation covers the fibre surface heterogeneity. While it has been found that negative charge on the surface of natural sheep fibre is distributed non-uniformly [51], the inhomogeneity is still enhanced by the radiation effect. As mentioned above, the Cr(III) complexes should always have the coordination number of 6 with the octahedral form [47]. Therefore, the presumed option of ligands for the Cr(III) is quasi-selective. If the Cr(III) cations do not find enough suitable ligands already on the fibre surface, they diffuse into the bulk. Inside, they interact with suitable ligands according to the spatial and wool structural conditions. On the other

hand, in the case of single Cu(II) adsorption, only the 24 kGy dosed sample satisfies the Freundlich model. This corresponds to the concept of an inhomogeneous surface disrupted by the critical dose of 24 kGy initiating the S-S bond breaking.

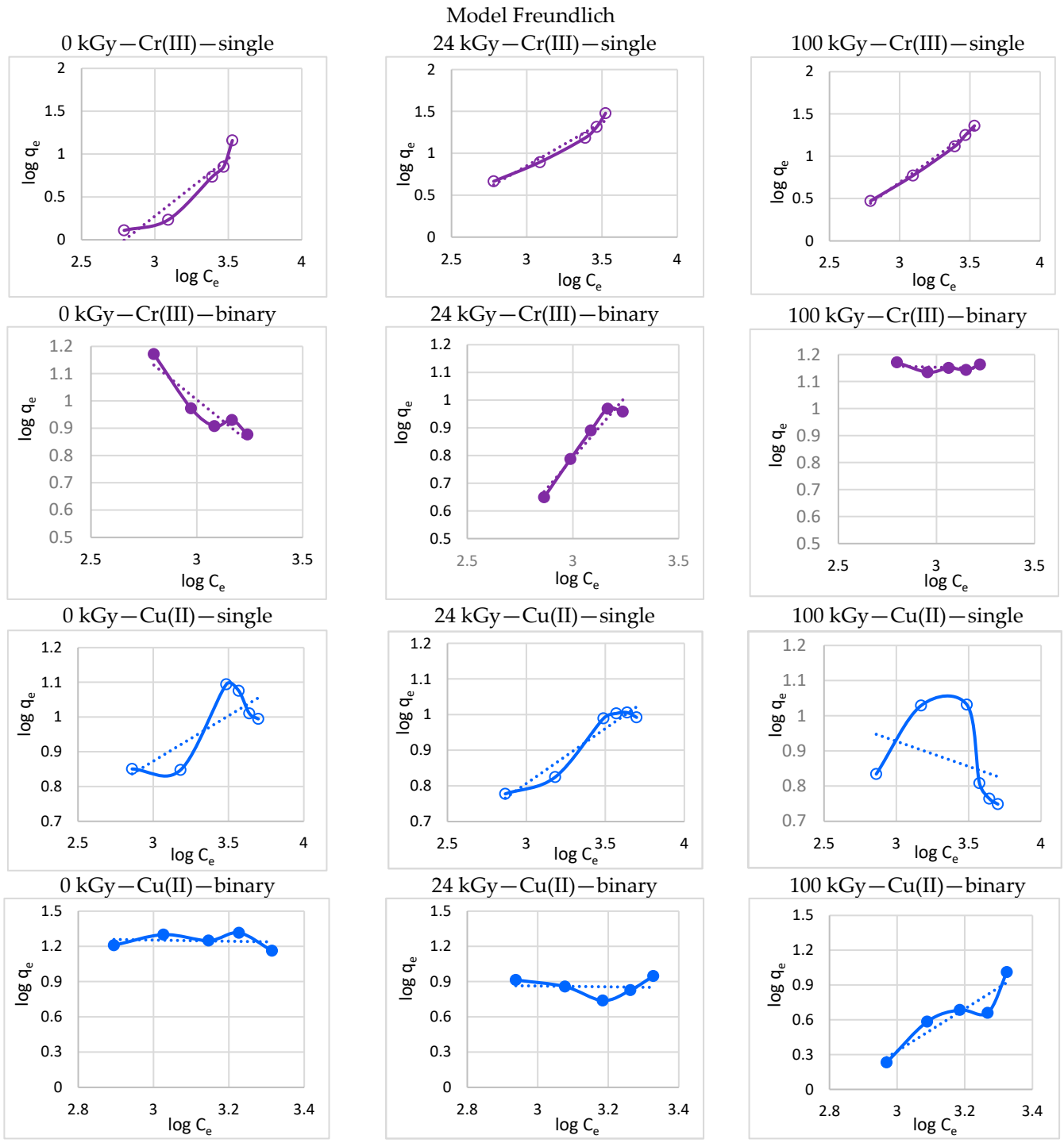

Figure 2. Freundlich charts of processed experimental data for Cr(III) and Cu(II) for both single and binary systems.

3.2.2. Adsorption from Binary Solutions

As regards the Cr(III) adsorption from the binary solution, conformity with the single system is consistent only for 24 kGy when the S-S bond disruption starts, while the 0 kGy sample is quasi-fitting. The 100 kGy dosed wool deviates from the model applicability fully.

This indicates that the predominance of the adsorbed Cr(III) over Cu(II) [35] in this sample leads to a more homogeneous layer formed mainly by the Cr(III)-complex, which reduces the assumptions of compliance with the Freundlich model.

On the contrary, the conformity for the Cu(II) adsorption from the binary system matches the Freundlich model just for the 100 kGy sample, even if only at the quasi-fitting level. However, it can be said that the fitting of the Cr(III) and the Cu(II) alternates in all binary samples; where the value of R^2 for one cation is smaller, for the other cation it is higher, and vice versa (Table 2). This observation corresponds to the competing adsorption position.

3.3. Dubinin–Radushkevich Model

The Dubinin–Radushkevich model is an empirical model. In general, it describes the adsorption mechanism with a Gaussian distribution of energy on a heterogeneous surface [52]. Figure 3 shows the course of individual dependencies.

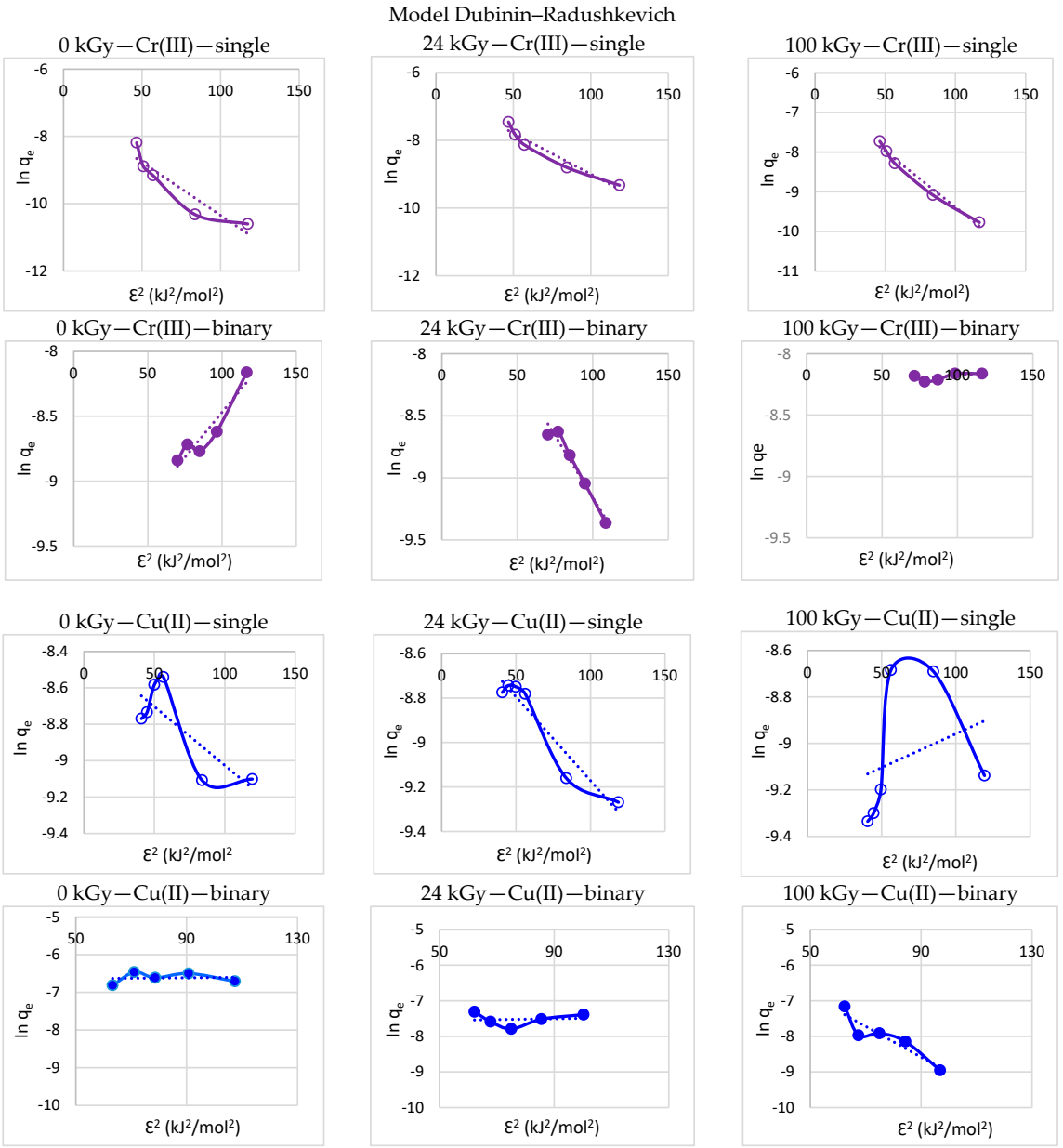

Figure 3. Dubinin–Radushkevich charts of processed experimental data for Cr(III) and Cu(II) for both single and binary systems.

3.3.1. Adsorption from Single Solutions

The model can be used to distinguish between physical and chemical adsorption. In our case, for single Cr(III), the native wool (0 kGy) fits the model at the quasi-fit level. We deduce that due to the specific coordination number of 6, the Cr(III) on the non-irradiated wool does not find enough opportunities to bind chemically; therefore, it binds by a mixed mechanism, mainly physically. Yet, for the 24 and 100 kGy samples, a satisfactory match can be observed. Here, the chemical mechanism also contributes to the physical one, thanks to the increasing cysteic acid, which binds the Cr(III) reactively as a salt.

The Cu(II) for 24 kGy shows some threshold fitting, but does not fit at all for 0 and 100 kGy, which indicates preferential chemisorption. For 24 kGy, we can admit a mixed mechanism, because this dose induces a very variable structure, as said above.

3.3.2. Adsorption from Binary Solutions

Adsorption of the Cr(III) in competitive conditions quasi-fits the model for the 0 kGy and fully for the 24 kGy samples, pursuant to the single system. This supports the conception of preferential physisorption of Cr(III) under these conditions in the binary system, too. Yet, for the 100 kGy dose, dependence does not fit at all, indicating that the Cr(III) physisorption for 0 and 24 kGy is already for 100 kGy suppressed by chemisorption. The reason may be that the content of the cysteic acid generated by the 100 kGy dose is already high enough also for chemical binding of the Cr(III) as cysteinate. Some part of the cysteic acid is also available for reaction with the Cu(II). This probably alleviates the deficit of the Gaussian energy distribution character.

On the contrary, the Cu(II) adsorption on 0 and 24 kGy samples does not fit at all and quasi-fits for 100 kGy. Thus, according to the Dubinin–Radushkevich model, the Cu(II) is bound on 0 and 24 kGy wool chemically, but not physically. On 100 kGy wool, the Cr(III) already competes with Cu(II) in chemisorption.

3.4. Temkin Model

The Temkin model relates adsorbent–adsorbate interactions. The model assumes the linearly decreasing heat of the adsorption of all molecules in the layer covering the surface. Simultaneously, the binding energies are distributed uniformly [53]. Related charts of the processed experimental data for the Cr(III) and the Cu(II) for both single and binary systems are displayed in Figure 4.

3.4.1. Adsorption from Single Solutions

As published [52], the model does not give the appropriate conformity for a complex adsorption system with a liquid phase. In our case of the **single** Cr(III), the Temkin model fits both the 0 kGy and 100 kGy samples on the quasi-fitting level (Table 2, Figure 4). Here, the situation approaches a linear decrease in the heat of adsorption and a more homogeneous distribution of binding energy due to the selective construction of Cr(III)-complexes. Even the 24 kGy sample is not much different from this one. The lower linearity of the heat decrease is related to the formation of two types of generated Cr(III)-complex, based on carboxylate and cysteinate.

On the other hand, the single Cu(II) meets the model pre-24 kGy, differing from 0 kGy and 100 kGy markedly. Adsorption on the 24 kGy sample indicates the fulfilment of the expected decrease in the heat of adsorption.

3.4.2. Adsorption from Binary Solutions

Unlike the single systems, the Cr(III) in the binary medium fits fully and exactly the 24 kGy sample, while the Cu(II) does not meet the correlation criterion at all. Those non-fitting cases are connected with the differentially distributed negative charge on the surface due to the different types of generated Cu(II)-complexes. In the case of the Cu(II), it seems that the adsorption capacity q_e for samples dosed with 0 kGy and 24 kGy depends very little on the initial concentration of Cu(II) in the binary solution (Figure 4).

3.5. Flory–Huggins Model

The Flory–Huggins model reflects the degree of the surface coverage of an adsorbent, which can characterize the feasibility and spontaneity of the adsorption [52]. Figure 5 presents dependencies constructed from our experimental results.

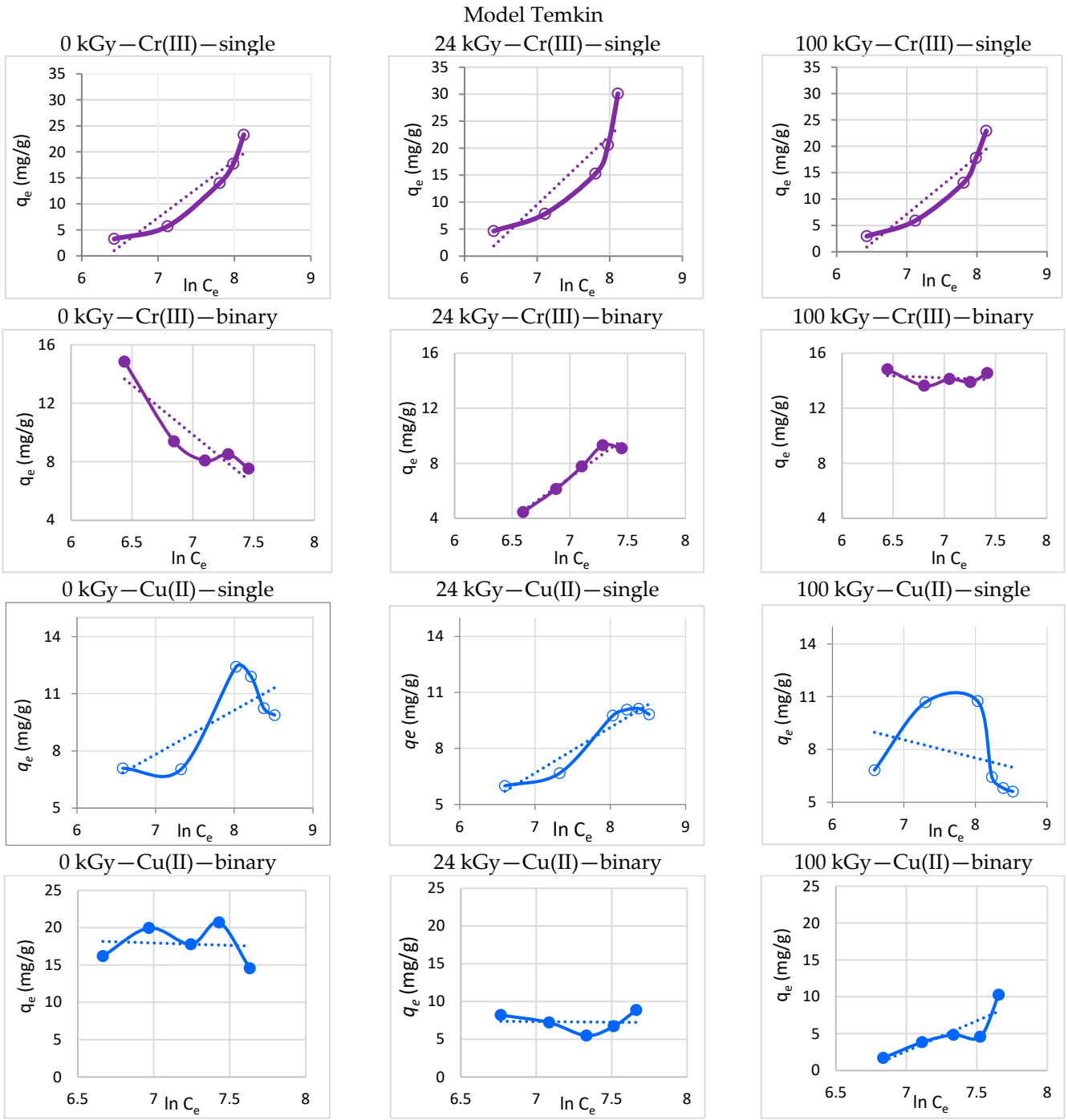

Figure 4. Temkin charts of processed experimental data for Cr(III) and Cu(II) for both single and binary systems.

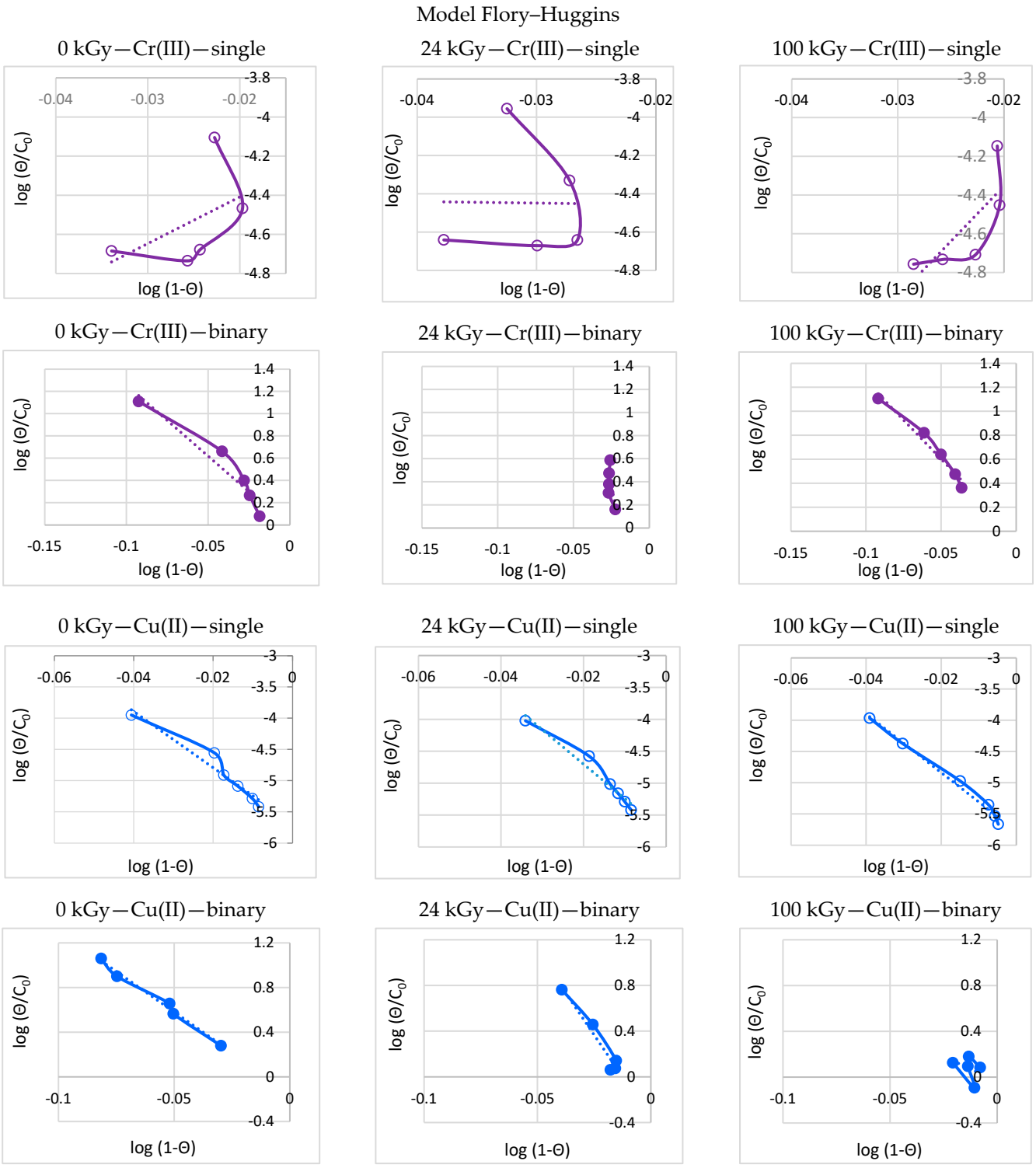

Figure 5. Flory–Huggins charts of processed experimental data for Cr(III) and Cu(II) for both single and binary systems.

3.5.1. Adsorption from Single Solutions

In the single systems, both cation Cr(III) and Cu(II) show entirely different results (Table 2, Figure 5). The Cr(III) does not meet the criterion anywise, in accordance with the concept of the selective selection of ligands, which are not sufficient on the surface to cover the surface with Cr(III)-complex. However, the Cu(II) fits completely for all

samples, with the potential to cover the entire available surface and indicating the process' spontaneity [34].

3.5.2. Adsorption from Binary Solutions

In the binary media, the Cr(III) shows surprisingly complying results for 0 and 100 kGy, unlike the single Cr(III). Since the Cu(II) simultaneously keeps the conformity for both 0 kGy and 24 kGy, we have to admit that the degree of the coverage and the spontaneity of the adsorption of harmonious samples is caused by the cooperative adsorption [40] of both partners. For the 100 kGy dosed sample with a higher content of cysteic acid, the connection with the above-mentioned fact that the Cr(III) affinity towards cysteic acid is superior to the Cu(II) in the binary solution can be assumed.

3.6. Halsey Model

The Halsey model provides suitable compliance with multilayer adsorption at a relatively large distance from the surface and when the adsorbent is of heterogeneous nature [54], as we consider wool. Figure 6 shows graphical dependencies for the Halsey model.

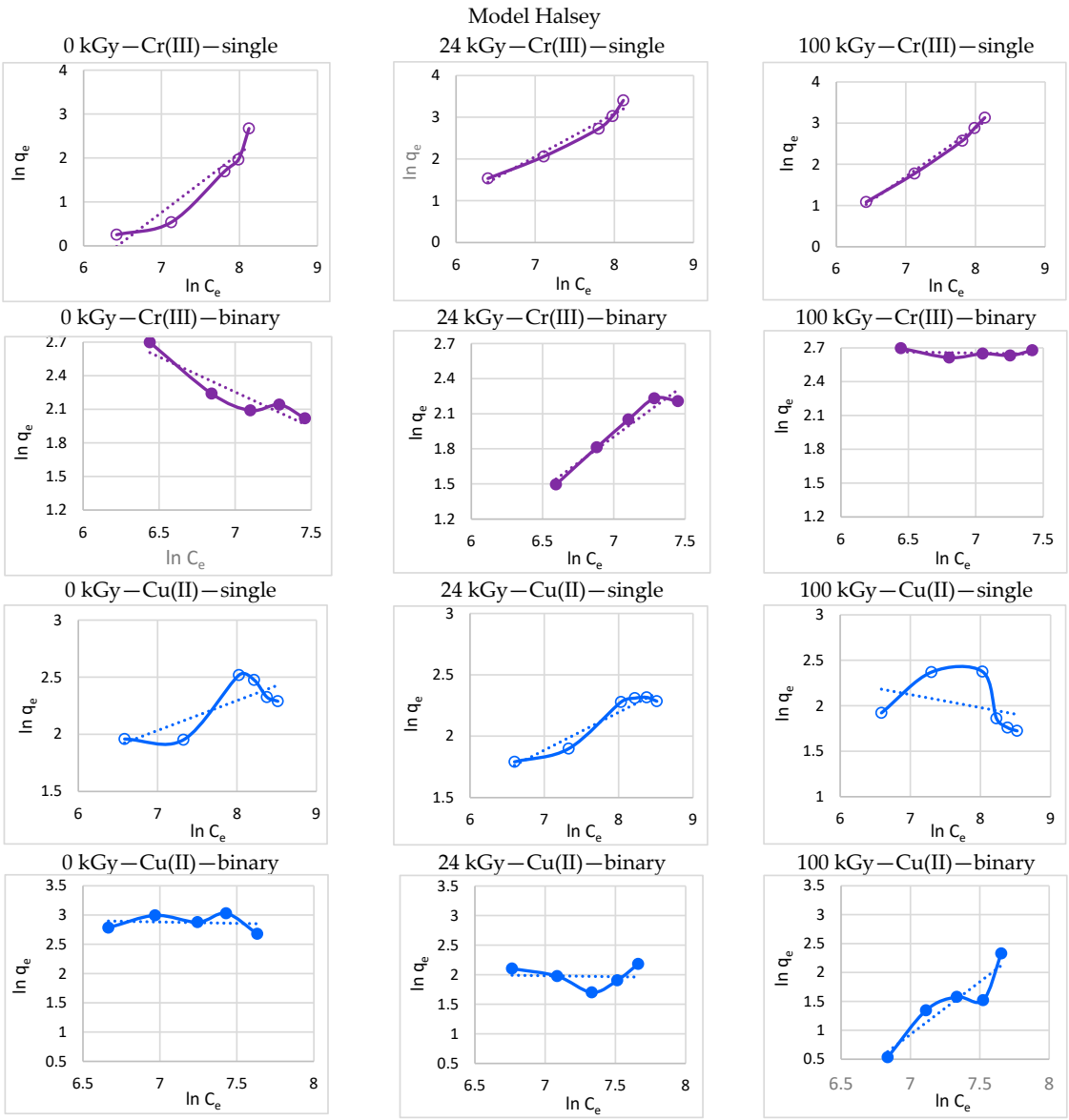

Figure 6. Halsey charts of processed experimental data for Cr(III) and Cu(II) for both single and binary systems.

3.6.1. Adsorption from Single Solutions

The single Cr(III) matches the model for 24 and 100 kGy and quasi-fits the native wool, implying a lower measure of heterogeneity compared to the exposed samples (Table 2, Figure 6). Because the Cr(III) forms the complexes selectively, the large distance of the complex from the surface could be fulfilled, too. The correlation observed indicates that in the case of the single Cu(II), the conformal criterion is calculated only for the 24 kGy sample, when the S-S starts to break and the variation of the charge occurs, as resulted from Equation (2).

3.6.2. Adsorption from Binary Solutions

In the binary systems, the tendency of the Cr(III) behaviour in the single system is kept, with the exception of 100 kGy dosed wool. Yet, the Cu(II) shows fully another tendency with quasi-fitting for the 100 kGy sample, when due to the irradiation, the wool heterogeneity is already enhanced enough to lead at least to a partial matching. It is noteworthy that the results for the Halsey model keep remarkably well the Freundlich isotherm for both single and binary systems. It is understandable since they are based on a similar principle.

3.7. Harkins–Jura Model

Multilayer adsorption on the surface of the adsorbent having a heterogeneous distribution of pores [32] is a prerequisite for the Harkins–Jura model. The ultrasonic scouring, to which the samples were subjected before the sorption experiments [35], disturbed the original surface of the fibres to some extent and created pores, as assumed by this model. In terms of surface heterogeneity, there is some similarity with the Halsey model. The respective dependencies are displayed in Figure 7.

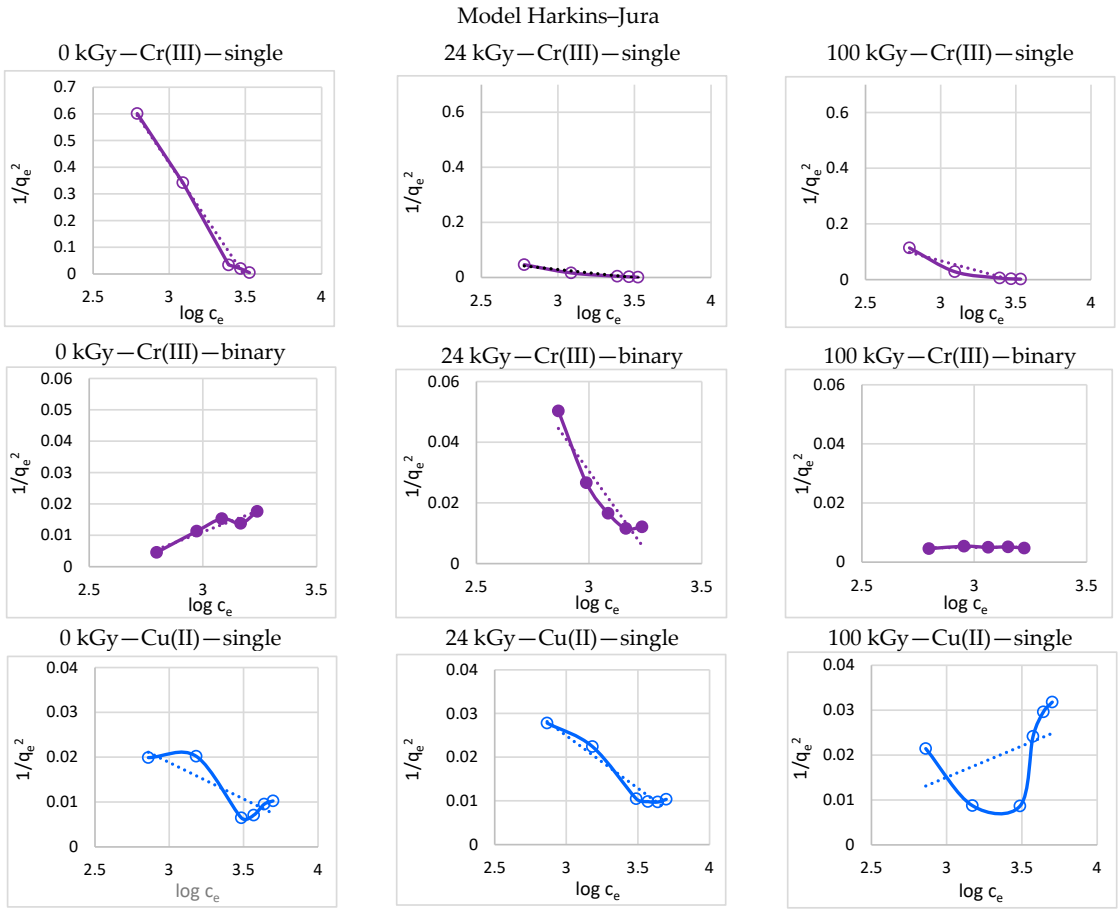

Figure 7. *Cont.*

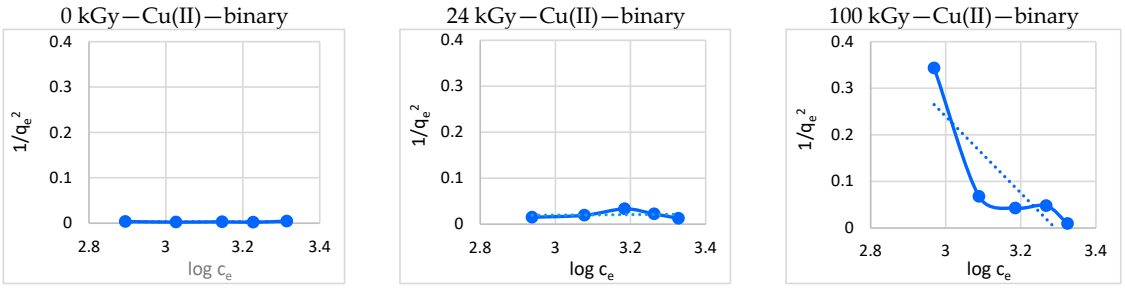

Figure 7. Harkins–Jura charts of processed experimental data for Cr(III) and Cu(II) for both single and binary systems.

3.7.1. Adsorption from Single Solutions

In the single system, the Cr(III) is approximately in conformity with the Halsey model (two full consonances and one quasi-fitting), and whole conformity is calculated for the single Cu(II) adsorption on the 24 kGy dosed wool (Table 2, Figure 7).

3.7.2. Adsorption from Binary Solutions

As for the binary systems, an approximate agreement with the Halsey isotherm is observed for the Cr(III), unlike the Cu(II), where the Cu(II) does not match at all. The observed differences may come from the fact that the Harkin–Jura model also takes into account pores on the adsorbent, which originate from the process of ultrasonic scouring and the irradiation of wool. Therefore, physisorption can also be applied here.

3.8. Jovanovic Model

A porous surface and the possibility of the adsorbate also binding physically are related to the Jovanovic model [55], in addition to the Langmuir model. Besides balanced relative rates of adsorption and desorption, this covers some surface binding vibrations. The correspondent dependencies for the Jovanovic model are presented in Figure 8.

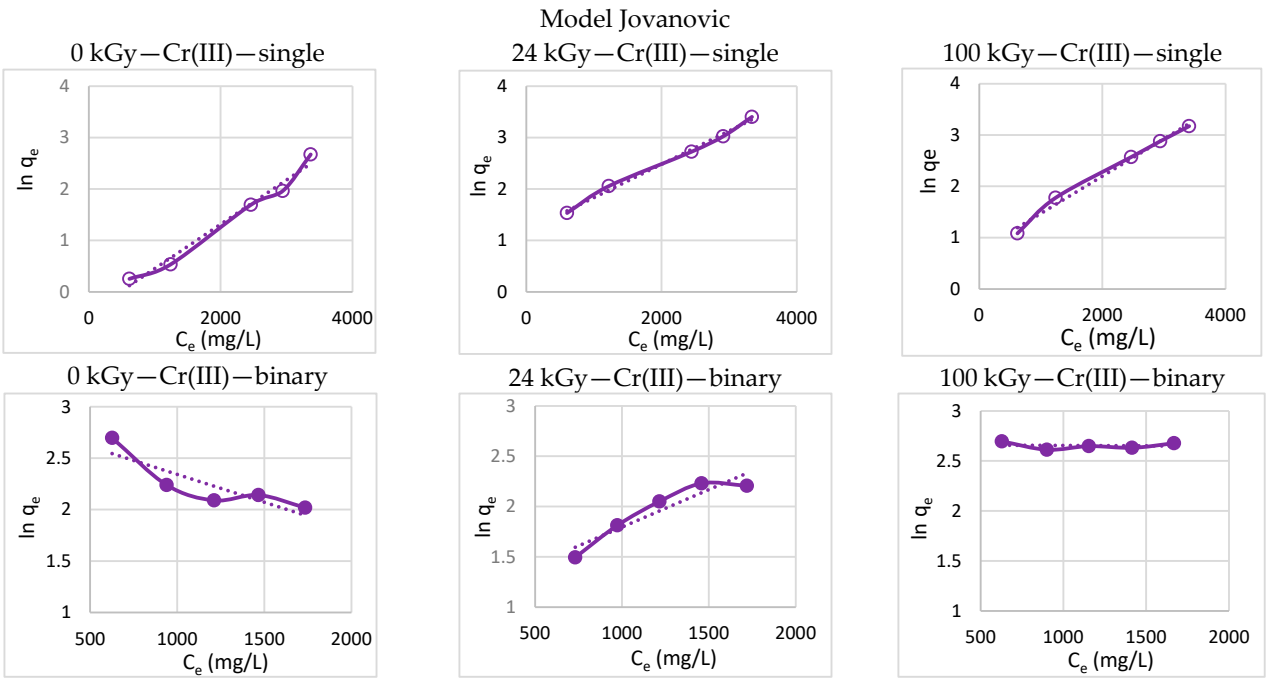

Figure 8. *Cont.*

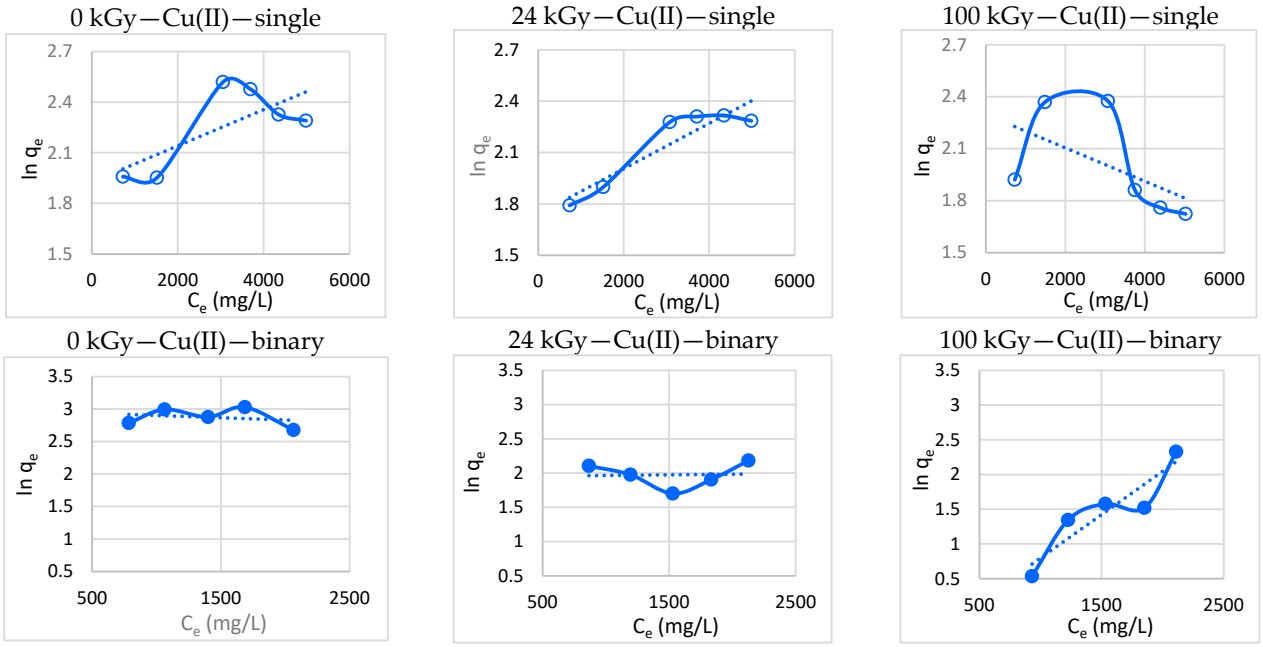

Figure 8. Jovanovic charts of processed experimental data for Cr(III) and Cu(II) for both single and binary systems.

3.8.1. Adsorption from Single Solutions

In the single Cr(III) solution, the cation meets the Jovanovic model fully (Table 2, Figure 8), regardless of the absorbed dose. Considering the Cr(III) coordination number of 6 and an octahedral form exclusively, the wool surface itself may not provide full saturation with the needed ligands, which leads to side physical interactions, as well. The electron beam not only increases the number of pores disrupting both the physical and chemical structure of the fibre, but also increases the amount of cysteic acid available to bind the Cr(III). These facts contribute to the model fitting. Unlike the Cr(III), the single Cu(II) meets the model only for 24 kGy at the quasi-fitting level, indicating that the Cu(II) prefers chemical interaction to physical interaction. In addition, the Cu(II) is not as picky in its choice of ligands, like the Cr(III).

3.8.2. Adsorption from Binary Solutions

In the binary solutions, the Cr(III) physical adsorption on the 0 kGy dosed wool is of little use since the Cu(II) preferentially covers the fibre surface as chemically bound. The Cr(III) adsorption on the 24 kGy dosed sample already quasi-fits the model, reflecting some disruption of the physical fibre structure. For the 100 kGy sample, the logarithm of the equilibrium adsorption q_e depends on the equilibrium concentration C_e negligibly indicating some saturation of the active points with Cr(III). If we take into account the higher affinity of the Cr(III) to the growing cysteic acid, as well as the increasing physical disruption of the fibre structure, the result for 100 kGy is not surprising. This can be attributed to the stronger competition of the Cr(III) for two reasons: the increasing number of pores created by the fibre disruption and, thus, better conditions for physical interaction, as well as the increasing content of cysteic acid, which manifests a higher affinity for the Cr(III) (see Section 3.2.1).

While the Cu(II) adsorption on the 0 and 24 kGy samples does not fit the model at all, for the 100 kGy sample the adsorption meets the model at the quasi-fitting level. Such data indicate that at the Cu(II) adsorption on the 0 and 24 kGy wool, there is no physical interaction alongside the predominance of the chemical bonding. Up to the 100 kGy sample, where fibre disruption is the highest, physical adsorption of Cu(II) is also applied to a lesser extent. The results for the adsorbed masses of both the cations from the binary system (see

Supplementary Materials) respond to these observations. If we accept this assumption, then the better agreement of the isotherm with the Jovanovic model, the more physical interactions are applied, and vice versa. Indeed, in competition with the Cr(III), the initially superior sorptivity of the Cu(II) decreased with the increasing dose; at the highest dose, a change of order in sorptivity was observed [35]. Comparing the correlation of both cations in the binary adsorption with this isothermal model shows a mirror image; an increase in the correlation of one cation is associated with a decrease in the other partner.

3.9. Elovich Model

The Elovich model predicts an exponential growth of adsorption sites when the adsorption and multilayer process occur [55]. The plots of the model for our results are displayed in Figure 9.

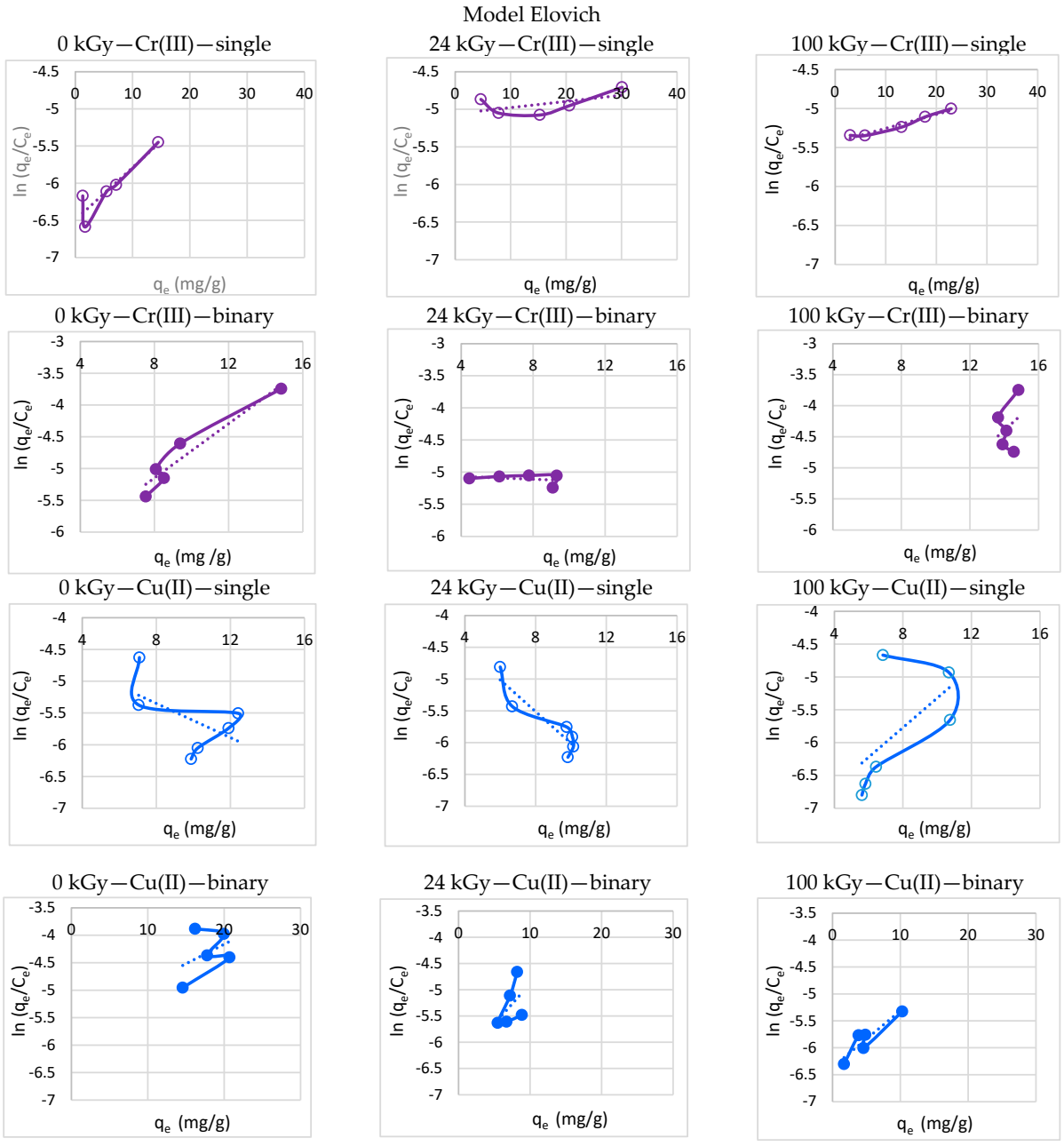

Figure 9. Elovich charts of processed experimental data for Cr(III) and Cu(II) for both single and binary systems.

3.9.1. Adsorption from Single Solutions

In the single system, this expectation is fulfilled for the Cr(III) on the 100 kGy dosed wool only (Table 2, Figure 9). As mentioned above, the higher the absorbed dose of energy, the more cysteic acid is produced. According to our assumption, just the Cr(III) has a higher affinity to cysteic acid, and that is why it matches the model when the amount of cysteic acid is high enough. On the other side, the Cu(II) shows an inadequate correlation level for all doses in question, which confirms our opinion about the better interaction of Cr(III)-cysteic acid. Being identical cations bonded on the fibre as complex salts, they cannot create the next adsorption points. Therefore, formation of a multilayer on the surface during adsorption from the single system is improbable.

3.9.2. Adsorption from Binary Solutions

But adsorption of the Cr(III) from the binary system on the 0 kGy sample meets the model. This fact can be explained applying the conception of cooperative adsorption for the Cr(III) when the Cu(II) is present in the primary layer, as mentioned in the Langmuir model. Such a state can be viewed as multilayer adsorption. Yet, on the 100 kGy dosed sample, cysteic acid is already available to react with the Cr(III), which may no longer be entirely dependent on cooperative adsorption with the Cu(II). Considering the Cu(II), only the 100 kGy sample gives matching at the quasi-fitting level in the binary system. We believe that here, the amount of cysteic acid is already enough to bind a terminal Cr(III) quantity, as well as some volume of the Cu(II). Therefore, the cooperative adsorption can be partially applied, affecting creation of the multilayer.

3.10. Redlich–Peterson Model

The Redlich–Peterson three-parameter model is a hybrid isotherm mixing the Langmuir and Freundlich isotherms. Therefore, it does not follow the ideal monolayer adsorption [52] and is applicable either on the homogeneous or heterogeneous surface. That is why one could expect the adsorption fitting for both cations from the single and binary media. Graphical results are shown in Figure 10.

3.10.1. Adsorption from Single Solutions

For the single Cr(III), the above mentioned supposition is not fulfilled at all (Table 2, Figure 10). It does not match the result for the Langmuir model and is also different from the Freundlich model. In general, to a great measure, we can consider the wool surface to be inhomogeneous because it contains several different functional groups capable of acting as active points. In addition, an uneven distribution of negative charge was detected there [51]. The electron irradiation complicates the situation even more. Yet, the single Cu(II) shows full conformity for all samples, just like the Langmuir model. Possibly, a strong predisposition of the Cu(II) to create various complexes is responsible for meeting the Redlich–Peterson supposition fully, regardless of the surface quality. Thus, the results for this model reflect chemisorption. In the case of the Cr(III), chemisorption is obstructed by the unavailability of the necessary selective ligands.

3.10.2. Adsorption from Binary Solutions

Adsorption from the binary solutions improves the conformity for the Cr(III) on the non-irradiated wool, as well as on the 100 kGy dosed one. On the other side, the Cu(II) adsorption fits only the non-irradiated sample at the quasi-fitting degree. From this point of view, it is consistent with the Langmuir model fitting. The partially favourable correlation with the Redlich–Peterson model for both cations at the native wool may originate from the above-mentioned cooperative adsorption, which did not occur at the specific 24 kGy sample. We attribute the agreement of the model for the adsorption of the Cr(III) on the 100 kGy sample to the increased content of cysteic acid, which preferentially reacts with the Cr(III).

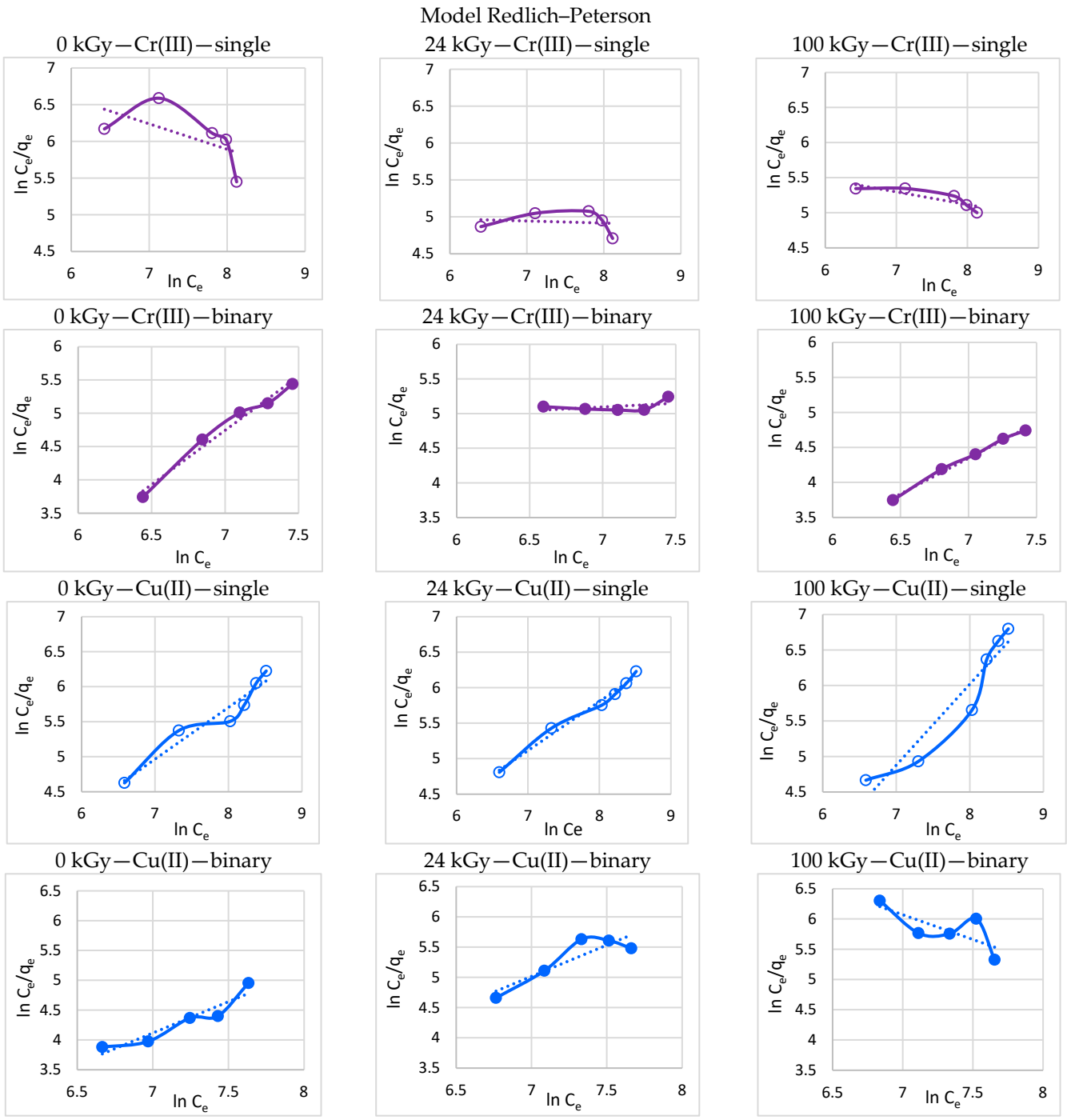

Figure 10. Redlich–Peterson charts of processed experimental data for Cr(III) and Cu(II) for both single and binary systems.

4. Conclusions

The experimental results of adsorption of the Cr(III) and the Cu(II) from single and binary solutions, with concentrations of each cation (15–35) mmol/L on electron-irradiated sheep wool with absorbed doses of (0-24-100) kGy, were preliminarily mathematically processed in the form of linearized equations for 10 isothermal models. The results' conformity with the selected models was evaluated using the correlation coefficient R^2 for linearized equations provided by the Excel program.

The presence of the competing cation in the binary solution significantly affected the course of all isotherms to the extent that even simultaneous fitting of the same cation in single and binary solutions is rare.

In the case of the Cr(III), 4 favourable matches were found out of 30 compared cases (Freundlich—24 kGy, Dubinin-Radushkevich—24 kGy, Halsey—24 kGy, and Harkins–Jura—0 kGy), while in the case of the Cu(II), only two (Flory–Huggins—0 and 24 kGy) were observed. It is concluded that the more regular structure of the Cr(III)-complex, supposing six ligands compared to the more variable structure of the Cu(II)-complex, is responsible for that. The competitive adsorption process also includes cooperative adsorption. Analysis of the isothermal models led to the conclusion that the adsorption of the Cr(III) in the presence of the Cu(II) is of chemical, as well as physical character, depending on the energy absorbed by the wool, while the adsorption of the Cu(II) is controlled preferentially by chemisorption.

The estimated obtained results have supported the conclusions of previous studies carried out with the corresponding single and binary solutions on wool modified by electron beam under identical conditions. The findings of this study will be the basis for choosing the optimal model, which will be subjected to a more detailed statistical analysis. Its conclusions can be used in designing a real material recycling process.

Supplementary Materials: The following supporting information can be downloaded at: https://www.mdpi.com/article/10.3390/pr11020502/s1, Table S1: Composition of both experimental and calibration Cr(III) solutions supplemented with Cu(II); Table S2: Composition of both experimental and calibration Cu(II) solutions supplemented with Cr(III); Table S3: Equilibrium sorptivity q_e for both Cr(III) and Cu(II); Table S4: Data for Cr(III) in binary system for graphic processing following Langmuir model; Table S5: Data for Cu(II) in binary system for graphic processing following Langmuir model; Table S6: Data for Cr(III) in binary system for graphic processing following Freundlich model; Table S7: Data for Cu(II) in binary system for graphic processing following Freundlich model; Table S8: Data for Cr(III) in binary system for graphic processing following Dubinin–Radushkevich model; Table S9: Data for Cu(II) in binary system for graphic processing following Dubinin–Radushkevich model; Table S10: Data for Cr(III) in binary system for graphic processing following Temkin model; Table S11: Data for Cu(II) in binary system for graphic processing following Temkin model; Table S12: Data for Cr(III) in binary system for graphic processing following Flory–Huggins model; Table S13: Data for Cu(II) in binary system for graphic processing following Flory–Huggins model; Table S14: Data for Cr(III) in binary system for graphic processing following Halsey model; Table S15: Data for Cu(II) in binary system for graphic processing following Halsey model; Table S16: Data for Cr(III) in binary system for graphic processing following Harkin–Jura model; Table S17: Data for Cu(II) in binary system for graphic processing following Harkin–Jura model; Table S18: Data for Cr(III) in binary system for graphic processing following Jovanovic model; Table S19: Data for Cu(II) in binary system for graphic processing following Jovanovic model; Table S20: Data for Cr(III) in binary system for graphic processing following Elovich model; Table S21: Data for Cu(II) in binary system for graphic processing following Elovich model; Table S22: Data for Cr(III) in binary system for graphic processing following Redlich–Peterson model; Table S23: Data for Cu(II) in binary system for graphic processing following Redlich–Peterson model.

Author Contributions: Conceptualization, M.P. and J.B.; Methodology, M.P. and J.B.; Formal Analysis, K.K.; Investigation, M.P., J.B. and K.K.; Writing—review & editing, M.P. All authors have read and agreed to the published version of the manuscript.

Funding: This research received no external funding.

Institutional Review Board Statement: Not applicable.

Informed Consent Statement: Not applicable.

Data Availability Statement: The datasets used and/or analyzed during the current study are available from the corresponding author upon reasonable request.

Conflicts of Interest: The authors declare no conflict of interest.

References

1. de Carvalho, R.P.; Chong, K.H.; Volesky, B. Evaluation of the Cd, Cu, and Zn Biosorption in Two-Metal Systems Using an Algal Biosorbent. *Biotechnol. Prog.* **1995**, *11*, 39–44. [CrossRef]
2. Chong, K.H.; Volesky, B. Metal Biosorption Equilibria in a Ternary System. *Biotechnol. Bioeng.* **1996**, *49*, 629–638. [CrossRef]
3. Al-Asheh, S.; Banat, F.; Al-Omari, R.; Duvnjak, Z. Predictitons of binary sorption isotherms for the sorption of heavy metals by pine bark using single isotherm data. *Chemosphere* **2000**, *41*, 659–665. [CrossRef]
4. Zheng, L.; Gao, Y.; Du, J.; Zhang, W.; Huang, Y.; Zhao, Q.; Duan, L.; Liu, Y.; Naidu, R.; Pan, X. Single and Binary Adsorption Behaviour and Mechanisms of Cd^{2+}, Cu^{2+} and Ni^{2+} onto Modified Biochar in Aqueous Solutions. *Processes* **2021**, *9*, 1829. [CrossRef]
5. Meng, Z.; Huang, S.; Ge, H.; Mu, W.; Lin, Z. Effects of competive adsorption with Ni(II) and Cu(II) on the adsorption of Cd(II) by modified biochar co-aged with acidic soil. *Chemosphere.* **2022**, *293*, e133621. [CrossRef]
6. Liang, Y.Q.; Li, H.; Mao, X.M.; Li, Y.; Wang, C.X.; Jin, L.Y.; Zhao, L.J. Competitive Adsorption of Methylene Blue and Cu(II) onto Magnetic Graphene Oxide/Alginate Beads. *Russ. J. Phys. Chem. A* **2020**, *94*, 2605–2613. [CrossRef]
7. Reynel-Avila, H.E.; Mendoza-Castillo, D.I.; Olumide, A.A.; Bonilla-Petriciolet, A. A survey of multi-component sorption models for the competitive removal of heavy metal ions using bush mango and flamboyant biomasses. *J. Mol. Liq.* **2016**, *224*, 1041–1054. [CrossRef]
8. Putro, J.N.; Santoso, S.P.; Ismadji, S.; Ju, Y.-H. Investigation of heavy metal adsorption in binary system by nanocrystalline cellulose-Bentonite nanocomposite: Improvement on extended Langmuir isotherm model. *Micropor. Mesopor. Mat.* **2017**, *246*, 166–177. [CrossRef]
9. Sun, X.; Huang, H.; Zhu, Y.; Du, Y.; Yao, L.; Jiang, X.; Gao, P. Adsorption of Pb^{2+} and Cd^{2+} onto Spirulina platensis harvested by polyacrylamide in single and binary solution systems. *Colloid Surf. Asp.* **2019**, *583*, e123926. [CrossRef]
10. Sellaoui, L.; Mendoza-Castillo, D.I.; Reynel-Ávilab, H.E.; Ávila-Camacho, B.A.; Díaz-Muñoz, L.L.; Ghalla, H.; Bonilla-Petriciolet, A.; Lamine, A.B. Understanding the adsorption of Pb^{2+}, Hg^{2+} and Zn^{2+} from aqueous solution on a lignocellulosic biomass char using advanced statistical physics models and density functional theory simulations. *Chem. Eng. J.* **2019**, *365*, 305–316. [CrossRef]
11. Ahmed, Z.; Wu, P.; Jiang, L.; Liu, J.; Ye, Q.; Yang, Q.; Zhu, N. Enhanced simultaneous adsorption of Cd(II) and Pb(II) on octylamine functionalized vermiculite. *Colloid Surf. A* **2020**, *604*, e125285. [CrossRef]
12. Dhiman, N. Binary adsorption of [Pb(II) + Co(II)] from aqueous solution using thiolated saw dust. *Water. Sci. Technol.* **2021**, *84*, 2591–2600. [CrossRef]
13. Babakhani, A.; Sartaj, M. Competitive adsorption of nickel(II) and cadmium(II) ions by chitosan cross-linked with sodium tripolyphosphate. *Chem. Eng. Commun.* **2021**, *209*, 1348–1366. [CrossRef]
14. Mahvi, A.H.; Nabizadeh, R.; Gholami, F.; Khairi, A. Adsorption of chromium from wastewater by *Platanus orientalis* leaves. *J. Environ. Health Sci. Eng.* **2007**, *4*, 191–196.
15. Gholami, F.; Mahvi, A.H.; Omrani, G.A.; Nazmara, S. Removal of chromium (VI) from aqueous solution by Ulmus leaves. *J. Environ. Health Sci. Eng.* **2006**, *3*, 97–102.
16. Wang, L.; Li, Z.; Wang, Y.; Brookes, P.C.; Wang, F.; Zhang, Q.; Xu, J.; Liu, X. Performance and mechanisms for remediation of Cd(II) and As(III) co-contamination by magnetic biochar-microbe biochemical composite: Competition and synergy effects. *Sci. Total. Environ.* **2021**, *750*, e141672. [CrossRef]
17. Balkaya, N.; Bektas, N. Chromium(VI) sorption from dilute aqueous solutions using wool. *Desalin. Water Treat.* **2009**, *3*, 43–49. [CrossRef]
18. Balköse, D.; Baltacioğlu, H. Adsorption of heavy metal cations from aqueous solutions by wool fibers. *J. Chem. Technol. Biot.* **1992**, *54*, 393–397. [CrossRef]
19. Ghosh, A.; Collie, S.R. Keratinous materials as novel absorbent systems for toxic pollutants. *Defence Sci. J.* **2014**, *64*, 209–221. [CrossRef]
20. Tirtom, V.N.; Goulding, Ş.; Henden, E. Application of a wool column for flow injection online preconcentration of inorganic mercury(II) and mercury species prior to atomic fluorescent measuremet. *Talanta* **2008**, *76*, 1212–1217. [CrossRef]
21. Aluigi, A.; Tonetti, C.; Vineis, C.; Tonin, T.; Mazzuchetti, G. Adsorption of copper(II) ions by keratin/PA6 blend nanofibres. *Eur. Polym. J.* **2011**, *47*, 1756–1764. [CrossRef]
22. Taddei, P.; Moniti, P.; Freddi, G.; Arai, T.; Tsukada, M. Binding of Co(II) and Cu(II) cations to chemically modified wool fibres: An IR investigation. *J. Mol. Struct.* **2003**, *650*, 105–113. [CrossRef]
23. Radetić, M.; Jocić, D.; Jovanovčić, P.; Rajaković, L.; Thomas, H.; Petrović, Z.L. Recycled-Wool-Based Nonwoven Material as a Sorbent for Lead Cations. *J. Appl. Polym. Sci.* **2003**, *90*, 379–386. [CrossRef]
24. Dakiky, M.; Khamis, M.; Manassra, A.; Mer'eb, M. Selective adsorption of chromium(VI) in industrial wastewater using low-cost abundantly available adsorbents. *Adv. Environ. Res.* **2002**, *6*, 533–540. [CrossRef]
25. Porubská, M.; Hanzlíková, Z.; Braniša, J.; Kleinová, A.; Hybler, P.; Fülöp, M.; Ondruška, J.; Jomová, K. The effect of electron beam on sheep wool. *Polym. Degrad. Stab.* **2015**, *111*, 151–158. [CrossRef]
26. Hanzlíková, Z.; Braniša, J.; Hybler, P.; Šprinclová, I.; Jomová, K.; Porubská, M. Sorption properties of sheep wool irradiated by accelerated electron beam. *Chem. Pap.* **2016**, *70*, 1299–1308. [CrossRef]
27. Hanzlíková, Z.; Braniša, J.; Jomová, K.; Fülöp, M.; Hybler, P.; Porubská, M. Electron beam irradiated sheep wool—Prospective sorbent for heavy metals in wastewater. *Sep. Purif. Technol.* **2018**, *193*, 345–350. [CrossRef]

28. Porubská, M.; Kleinová, A.; Hybler, P.; Braniša, J. Why Natural or Electron Irradiated Sheep Wool Show Anomalous Sorption of Higher Concentrations of Copper(II). *Molecules* **2018**, *23*, 3180. [CrossRef]
29. Braniša, J.; Kleinová, A.; Jomová, K.; Malá, R.; Morgunov, V.; Porubská, M. Some Properties of Electron Beam-Irradiated Sheep Wool Linked to Cr(III) Sorption. *Molecules* **2019**, *24*, 4404. [CrossRef]
30. Braniša, J.; Kleinová, A.; Jomová, K.; Weissabel, R.; Cvik, M.; Branišová, Z.; Porubská, M. Sheep Wool Humidity under Electron Irradiation Affects Wool Sorptivity towards Co(II) Ions. *Molecules* **2021**, *26*, 5206. [CrossRef]
31. Hanzlíková, Z.; Lawson, M.K.; Hybler, P.; Fülöp, M.; Porubská, M. Time-Dependent Variations in Structure of Sheep Wool Irradiated by Electron Beam. *Adv. Mater. Res.* **2017**, *2017*, 3849648. [CrossRef]
32. Braniša, J.; Jomová, K.; Kovalčíková, R.; Hybler, P.; Porubská, M. Role of Post-Exposure Time in Co(II) Sorption of Higher Concentrations on Electron Irradiated Sheep Wool. *Molecules* **2019**, *24*, 2639. [CrossRef] [PubMed]
33. Braniša, J.; Jomová, K.; Lapčík, Ľ.; Porubská, M. Testing of electron beam irradiated sheep wool for adsorption of Cr(III) and Co(II) of higher concentrations. *Polym. Test.* **2021**, *99*, 107191. [CrossRef]
34. Porubská, M.; Jomová, K.; Lapčík, Ľ.; Braniša, J. Radiation-modified wool for adsorption of redox metals and potentially for nanoparticles. *Nanotechnol. Rev.* **2020**, *9*, 1017–1026. [CrossRef]
35. Braniša, J.; Koóšová, K.; Lendelová, K.; Porubská, M. Competitive adsorption of Cr(III) and Cu(II) on electron irradiated sheep wool from binary solution can be controlled by absorbed dose. *ACS Omega* **2022**, *7*, 38015–38024. [CrossRef]
36. Langmuir, L. The adsorption og fases on plane surfaces of glass, mica and platinum. *J. Am. Chem. Soc.* **1918**, *40*, 1361–1403. [CrossRef]
37. Freundlich, H. Über die adsorption in lösungen. *Z. Phys. Chem.* **1907**, *57*, 385–470. [CrossRef]
38. Dubinin, M.M. The potential theory of adsorption of gases and vapors for adsorbents with energetically non-uniform surface. *Chem. Rev.* **1960**, *60*, 235–266.
39. Temkin, M.I.; Pyzhev, V. Kinetics of ammonia synthesis on promoted iron catalyst. *Acta Phys. Chim. USSR* **1940**, *12*, 327–356.
40. Flory, P.J. Thermodynamics of High Polymer Solutions. *J. Chem. Phys.* **1942**, *10*, 51–61. [CrossRef]
41. Halsey, G.; Taylor, H.S. The adsorption of hydrogen on tungsten powders. *J. Chem. Phys.* **1947**, *15*, 624–630. [CrossRef]
42. Harkins, W.D.; Jura, G. An Adsorption Method for the Determination of the Area of a Solid without the Assumption of a Molecular Area, and the Area Occupied by Nitrogen Molecules on the Surfaces of Solids. *J. Chem. Phys.* **1943**, *11*, 431–432. [CrossRef]
43. Jovanovic, D.S. Physical adsorption of gases. I. Isotherms for monolayer and multilayer adsorption. *Kolloid Z. Z. Polym.* **1969**, *235*, 1203–1213. [CrossRef]
44. Elovich, S.Y.; Larionov, O.G. Theory of adsorption from nonelectrolyte solutions on solid adsorbents. *Bull. Acad. Sci. USSR Div. Chem. Sci.* **1962**, *11*, 198–203. [CrossRef]
45. Redlich, O.; Peterson, D.L. A useful adsorption Isotherms. *J. Chem. Phys.* **1959**, *63*, 1024–1027. [CrossRef]
46. Nikiforova, T.E.; Kozlov, V.A.; Sionikhina, A.N. Peculiarities of sorption of copper(II) ions by modified wool keratin. *Prot. Met. Phys. Chem.* **2019**, *55*, 849–857. [CrossRef]
47. Šima, J.; Koman, M.; Kotočová, A.; Segľa, P.; Tatarko, M.; Valigura, D. *Anorganická Chémia*, 2nd ed.; STU: Bratislava, Slovakia, 2011; pp. 375–378. (In Slovak)
48. Baryshnikova, A.T.; Minaev, B.F.; Baryshnikov, G.V.; Sun, W.H. Quantum-chemical study of the structure and magnetic properties of mono- and binuclear Cu(II) complexes with 1,3-bis(3-(pyrimidin-2-yl)-1H,-1,2,4-triazol-5-yl)propane. *Russ. J. Inorg. Chem.* **2016**, *61*, 588–593. [CrossRef]
49. Chesnut, D.B.; Quin, L.D. Nature of Bonding in the Sulfuryl Group. *J. Comput. Chem.* **2004**, *25*, 734–738. [CrossRef]
50. Liu, S. Cooperative adsorption on solid surfaces. *J. Colloid Interface Sci.* **2015**, *450*, 224–238. [CrossRef]
51. Zimmerman, B.; Chow, J.; Abbott, A.G.; Ellison, M.S.; Kennedy, M.S.; Dean, D. Variation of Surface Charge along the Surface of Wool Fibers Assessed by High-Resolution Force Spectroscopy. *J. Eng. Fiber. Fabr.* **2011**, *6*, 61–66. [CrossRef]
52. Foo, K.Y.; Hameed, B.H. Insights into the modeling of adsorption isotherm systems. *Chem. Eng. J.* **2010**, *156*, 2–10. [CrossRef]
53. Hamdaoui, O.; Naffrechoux, E. Modeling of adsorption isotherms of phenol and chlorophenols onto granular activated carbon. Part I. Two-parameter models and equations allowing determination of thermodynamic parameters. *J. Hazard. Mater.* **2007**, *147*, 381–394. [CrossRef] [PubMed]
54. Amin, M.T.; Alazba, A.; Shafiq, M. Adsorptive removal of reactive Black 5 from wastewater using bentonite clay: Isotherms, kinetics and thermodynamics. *Sustainability* **2015**, *7*, 15302. [CrossRef]
55. Farouq, R.; Yousef, N.S. Equilibrium and kinetics studies of adsorption of copper(II) ions on natural biosorbent. *Int. J. Chem. Eng. Appl.* **2015**, *6*, 319–324. [CrossRef]